Hexacyanoferrate(III) Transport in Coated Montmorillonite Clay Films. Effects of Water-Soluble Polymers

Jean-Marie Séquaris

Institute of Applied Physical Chemistry (ICG 7), Research Centre Jülich, P.O. Box 1913, D-52425 Jülich, Germany

Received May 7, 1999. In Final Form: August 16, 1999

Hexacyanoferrate(III) $Fe(CN)_6^{3-}$, transport through coated montmorillonite clay films at a platinum electrode is studied with the cyclic voltammetric method. Experimental conditions are first established guaranteeing voltammetric detection based on a linear diffusion in the clay film. The square of the ratio (R^2) of current intensities obtained at the clay modifed electrode (CME) and the bare Pt electrode measures the relative variation of the $Fe(CN)_6^{3-}$, diffusion coefficient in the clay film. Thus, the effects of bathing electrolyte concentrations on R^2 are investigated and related to the swelling properties of the montmorillonite clay characterized by X-ray diffraction and sedimentation volume results. According to an applied model for the electric conductivity of montmorillonite clay solution, a relationship between the formation factor $F = 1/R^2$, the shape factor (α), and the clay film effective porosity (Φ_e) is established. The shape factor (α) includes orientation and axial ratio (the ratio (A/B) of the major axis (A) to the minor axis (B)) parameters which characterize the arrangement of montmorillonite particles in the clay film. The determination of Φ_e is based on relative variations of the sedimentation volumes. In a salt concentration range from 0.02 to 1 M NaCl, it can be thus proposed that an interparticle $Fe(CN)_6^{3-}$ transport in the clay film is limited by occluded montmorillonite particles with a constant axial ratio. The effects of water-soluble polymers on the shape factor (α), of montmorillonite particles are investigated. At polymer concentrations ≤5% (polymer to montmorillonite, w/w), nonionic poly(vinylpyrrolidone) (PVP) decreases $Fe(CN)_6^{3-}$ transport in CME while interactions with a low-molecular-weight poly(acrylic acid) (PAA) increases it. The polymer modifications of the clay film can be thus modeled. An aggregation with PVP favors a lateral formation of a band-type network with an increase of the particle axial ratio, i.e., lengthening of the interparticle transport pathway in the clay film. In the case of low-molecular-weight PAA, a specific adsorption at the edge of montmorillonite platelets induces an apparent decrease of the particle axial ratio. This can be related to an electrostatic stabilization of clay platelets stacked in a column model, which shortens the interparticle transport pathway in the clay film.

Introduction

The presence of clay minerals in soil or sediments is of considerable significance in the transport mechanisms of nutritients and environmental pollutants.[1] Indeed, the colloidal behavior of these anisometric, plate-shaped particles (<2 μm), their relatively high surface area, and differential swelling properties[2] control the fate of dissolved molecular species by adsorption processes at their surfaces or by limiting water transport. Thus, clay films deposited on the surface of soil pore walls have been shown to affect ion diffusion.[3] Clay walls and liners are often used for sealing off waste disposals.[4]

In this regard, the application of cyclic voltammetry (CV)[5−14] has opened up new approaches in the study of transport mechanism on a μm scale through clay films deposited at an electrode surface. Thus, anionic redox species such as hexacyanoferrate(III), ($Fe(CN)_6^{3-}$), which are electrostatically repelled by the negatively charged clay mineral surface, can be used as a conservative electrochemical marker to probe the diffusion pathway in clay films coating a platinum electrode.[8−14] Depending on the time window of the cyclic voltammetric method, monitored by the potential scan rate, it has been demonstrated that an effective diffusion coefficient for $Fe(CN)_6^{3-}$, can be determined inside the clay film of a clay-modified electrode (CME).[9−10] It follows that the ratio of the current intensity obtained at a CME and at a bare electrode can be utilized for information about the porous structure of the clay film.[9,12] Thus, the effects of the nature and concentration of bathing electrolytes on the CME permeability have been related to the swelling properties of the clay matrix. A direct relation between the clay platelet interlayer dimensions of montmorillonite[9] and the electrochemical responses can be established. In the case of a nonswelling clay mineral, kaolinite, a diffusive transport of $Fe(CN)_6^{3-}$, between particles or through pinholes in the clay film is suggested.[13]

In this work, the porosity parameter has been further considered in transport modeling by comparing the voltammetric behavior of CME with the swelling dependence of montmorillonite on the electrolyte concentration. Results from sedimentation volume experiments are thus taken into account in the estimation of an effective porosity of the clay film for $Fe(CN)_6^{3-}$ transport. The axial ratio

(1) Parker, A., Rae, J. E., Eds. *Environmental Interactions of Clays*; Springer: Berlin, 1998.
(2) Lagaly, G. In *Surfactant Sciences Series*, Vol. 47, Dobiás, B., Ed.; M. Dekker: New York, 1993, Chapter 10.
(3) Chen, S.; Franklin, R. E.; Johnson, A. D. *Soil Science* **1997**, *162*, 91.
(4) Weiss, A. *Appl. Clay Sci.* **1989**, *4*, 193.
(5) Ege, D.; Ghosh P. K.; White J. R.; Equey J.-F.; Bard A. J. *J. Am. Chem. Soc.* **1985**, *107*, 5644.
(6) Itaya K.; Bard A. J. *J. Phys. Chem.* **1985**, *89*, 5565.
(7) Liu H−Y.; Anson F. C. *J. Electroanal. Chem.* **1985**, *184*, 411.
(8) Fitch, A. *Clays Clay Miner.* **1990**, *38*, 391.
(9) Lee, S. A.; Fitch, A. *J. Phys. Chem.* **1990**, *94*, 4998.
(10) Fitch, A.; Du, Jia. *J. Electroanal. Chem.* **1991**, *319*, 409.
(11) Subramanian, P.; Fitch, A. *Environ. Sci. Technol.* **1992**, *26*, 1775.
(12) Fitch, A. In *Access in Nanoporous Materials*; Pinnavaia, T. J., Thorpe, M. F., Eds.; Plenum Press: New York, 1995; p 93.
(13) Stein, J. A.; Fitch, A. *Clays Clay Miner.* **1996**, *44*, 381.
(14) Joo, P.; Fitch, A.; Park, S.-H. *Environ. Sci. Technol.* **1997**, *31*, 2186.

10.1021/la990550e CCC: $19.00
Published on Web 12/04/1999

of montmorillonite particles, i.e., the ratio (A/B) of the major axis (A) to the minor axis (B) is also considered in the interpretation where the term "particle" can also designate an aggregation of single montmorillonite platelets.

In the same way, the effects of water-soluble polymers on the diffusional properties of clay films have been also investigated. Indeed, the interactions of natural[15,16] or synthetic[17−20] organic macromolecules with clay minerals are of great importance in stabilizing the soil structure. Microscopic modifications of the clay mineral particle surface properties by polymers[21] can affect the stability of the macroscopic soil aggregates through flocculation and dispersion phenomena depending on the polymer nature.

Materials and Methods

Materials. $K_3Fe(CN)_6$ and poly(acrylic acid) PAA with a molecular weight of 2000 g/mol were supplied by Aldrich (Germany). Poly(vinylpyrrolidone) (PVP) with different molecular weights, 5000 (K12), 44 000 (K30) and 400 000 (K80) g/mol was supplied by BASF, (Germany).

Na-montmorillonite I and II were prepared from Ca-bentonite (Süd-Chemie, Germany). Their cation exchange capacity (CEC) and BET are 98.1 meq/g and 88.7 m^2/g for Na-montmorillonite I and 87.5 meq/g and 95.9 m^2/g for Na-montmorillonite II respectively. From photon correlation spectroscopy (PCS) measurements, average equivalent spherical hydrodynamic diameters of 0.6 μm and 0.45 μm are calculated for Na-montmorillonite I and Na-montmorillonite II respectively in water. Polymer-modified montmorillonite suspensions were prepared by adding polymers to a 40 g/L Na-montmorillonite suspension up to a final concentration of 0.1, 0.5, 1, and 2 g/L. The solutions with added polymer were equilibrated for 65 h on a horizontal shaker at room temperature.

Methods. *Electrochemistry*. Voltammetric measurements of $Fe(CN)_6^{3-}$, were performed with a BAS-100A electrochemical analyzer. A Metrohm Pt disk electrode with a diameter of 3 mm served as the working electrode. A saturated calomel electrode (SCE) was used as a reference electrode and a platinum wire served as the auxiliary electrode. A 20 mL Metrohm cell thermostated at 20 °C was employed in these experiments.

Before any measurement, the Pt-electrode surface was briefly polished with a wet filter paper onto which some 0.3 μm abrasive grains had been sprayed. After rinsing with distilled water, the electrode was then dried by touching the surface with a soft absorbent paper tissue. The quality of the Pt electrode surface was tested by repeating (4 times) cyclic voltammograms from +0.6 V to −0.2 V (vs SCE) of 4 mM $Fe(CN)_6^{3-}$, dissolved in the bathing electrolyte solution of interest. In the case of a reproducibility of better than 98%, the measured reduction peak current intensity $I_{p_{sol}}$ was saved for further calculations (see Results section). After rinsing the Pt electrode with distilled water and drying, the clay-modified electrode (CME) was then prepared by transferring 2 μL of the Na-montmorillonite water dispersion (10−40 g/L) to the surface of the Pt electrode. The coating was allowed to dry by rotating the Pt electrode at 1000 rpm for 30 min. The CME was thus dipped into the electrolyte solution containing 4 mM $Fe(CN)_6^{3-}$, and programmable time-controlled recording voltammograms from +0.6 V to −0.2 V (vs SCE) were generally performed with a potential sweep rate of 0.05 V/s during a bathing time of up to 16 min i.e., when no time dependence is observed. At this response time, the corresponding reduction peak current intensities $I_{p_{CME}}$ were saved for further calculations (see Results section).

X-ray Diffraction. X-ray diffraction measurements were performed with with an X-ray diffractometer XRD 3000 TT Seifert (Germany). A homemade Pt disk surface of 6 mm diameter was used as a sample carrier where 20 μL of a 40 g/L Na-montmorillonite water suspension is deposited. As for CME preparation, this removable clay-modified Pt disk surface was allowed to rotate at 1000 rpm for 40 min. Under these drying conditions, a clay fim thickness of 6 ± 1 μm can be estimated by microscopy. A well-defined diffraction line at 1.29 ± 0.04 nm (d_{001}) was measured by XRD.[22−24] Effects of electrolyte solutions 0.5, 1, 2, and 4 M NaCl on the d_{001} diffraction line were observed by the addition of 20 μL of the corresponding electrolyte solution. The montmorillonite samples were then covered by a Mylar window film (Spex, US) for XRD analysis.

Sedimentation Volume. Sedimentation volume measurements were performed by adding the electrolyte solution in a range from 0.02 to 4 M NaCl in conical 10 mL vessels containing the preweighted dry montmorillonite (final montmorillonite concentrations were 10, 20, and 40 g/L). The suspensions were first equilibrated on a horizontal shaker at room temperature. After a shaking time of 24 h, the sedimentation tubes were then set upright to read the sedimentation volumes for a period of up to six months. The average sedimentation volumes expressed in cm^3/g were calculated from a linear regression analysis of the results after this period. It must be noted that in the presence of NaCl concentration ≥ 0.1 M, no sedimentation volume variation can be observed after 3 weeks.

Polymer-modified montmorillonites were obtained after drying the centrifugates (20 000 rpm, 30 min) of equilibrated 40 g/L Na montmorillonite suspensions at 60 °C in the presence of 2 g/L polymers.

Photon Correlation Spectroscopy. The photon correlation spectroscopy (PCS) measurements were performed using a Malvern ZetaSizer 4 equipped with a 5 mW He−Ne laser. Measurements were made at an angle of 90° with a particle concentration of 0.2 g/L. The monomodal cumulants method of the ZetaSizer 4 software was used to analyze the correlation function. An averaged translational diffusion constant is thus obtained, from which an equivalent spherical hydrodynamic diameter ($\bar{d}_z$) for the particle is calculated.

Viscosity. Viscometry measurements of Na-montmorillonite were made by using an Ubbelohde type capillary viscometer at 20 °C (Capillary Type 531 01/0a from Schott, Germany) with automatic measuring equipment (AVS 310) from Schott-Geräte. Flow time readings at three clay concentrations (0.5, 0.67, and 1 g/L) in water were repeated at least 5 times.

The axial ratio (A/B) of Na-montmorillonite particle, assimilated to oblate spheroids (ellipsoid of revolution about minor axis B with major axis $A \gg B$), was calculated from the intrinsic viscosity [η] according to the relation[25,26]

$$[\eta] = \lim_{\varphi \to 0} \frac{\eta_{sp}}{\varphi} = \frac{4}{3} \frac{A/B}{\tan^{-1}(A/B)} \approx 0.849 \frac{A}{B} \qquad (1)$$

where η_{sp} is the specific viscosity. The volume fraction of clay in solution, φ, is thus defined

$$\varphi = \left(\frac{c}{\rho_c}\right)(1 + \theta) \qquad (2)$$

where ρ_c is the mass density of the dry clay (2.7 g/cm^3), c is the

(15) Schnitzer, M. In *Environmental Impact of Soil Component Interactions*; Huang, P. M., Berthelin J., Bollag, J.-M., McGill, W. B., Page, A. L.; Eds.; CRC Press: Boca Raton, FL, 1995; p 3.

(16) Chenu, C. In *Environmental Impact of Soil Component Interactions*; Huang, P. M., Berthelin J., Bollag, J.-M., McGill, W. B., Page, A. L., Eds.; CRC Press: Boca Raton, FL, 1995; p 217.

(17) Ben-Hur, M.; Malik, M.; Letey, J.; Mingelgrin, U. *Soil Science* **1992**, *153*, 349.

(18) Lentz, R. D.; Shainberg, I.; Sojka, R. E.; Carter, D. L. *Soil Sci. Soc. Am. J.* **1992**, *56*, 1926.

(19) Ben-Hur, M.; Keren, R. *Soil Sci. Soc. Am. J.* **1997**, *61*, 565.

(20) Aase J. K.; Bjorneberg, D. L.; Sojka, R. E. *Soil Sci. Soc. Am. J.* **1998**, *62*, 1681.

(21) Theng, B. K. G. *Formation and Properties of Clay−Polymer Complexes*, Elsevier: Amsterdam, 1979.

(22) Norrish, K.; Rausell-Colom, J. A. *Clays Clay Miner.* **1963**, *10*, 123.

(23) Lagaly, G.; Schön, G.; Weiss, A. *Kolloid-Z. u. Z. Polymere* **1972**, *250*, 667.

(24) Slade, P. G.; Quirk, J. P.; Norrish, K. *Clays Clay Miner.* **1991**, *39*, 234.

(25) Kahn, A. *Clays Clay Miner.* **1959**, *6*, 220.

(26) Dufey, J. E.; Banin, A. *Soil Sci. Soc. Am. J.* **1979**, *43*, 782.

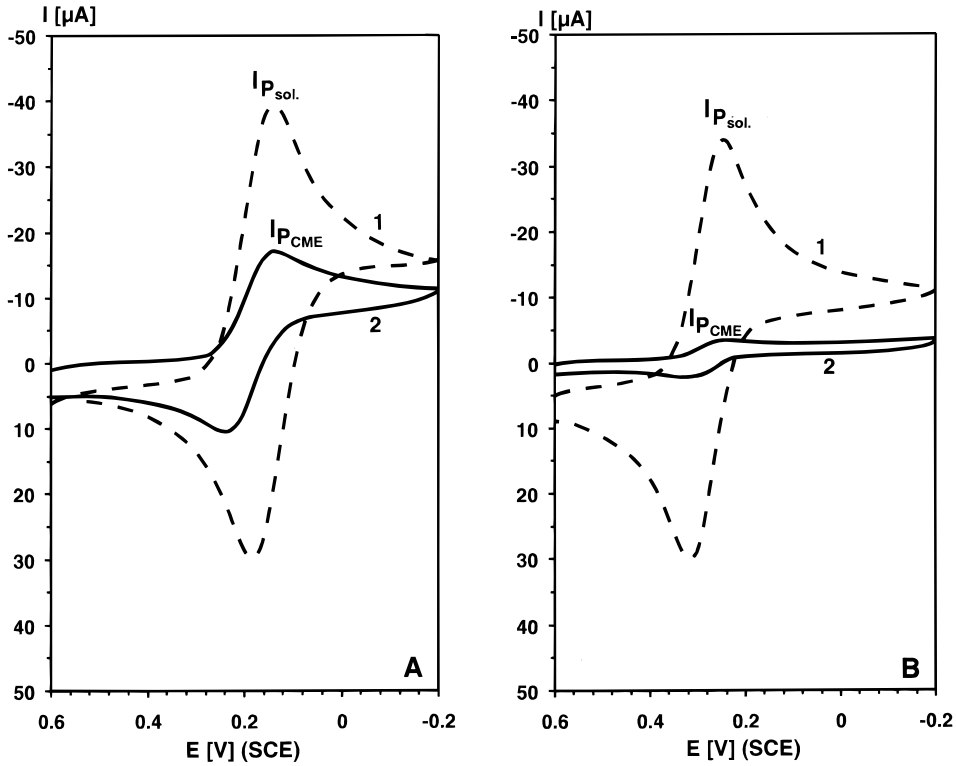

Figure 1. Cyclic voltammetric responses of $Fe(CN)_6^{3-}$ at montmorillonite clay modified electrode (CME) in 0.2 M NaCl (A) and 4 M NaCl (B) solutions. 1: bare Pt electrode; 2: CME; potential scan rate 0.05 V/s; CME coating 1.13 mg/cm^2; $K_3Fe(CN)_6$, 4 mM; Na-montmorillonite II.

concentration of clay, and θ is the immobilized water volume to clay volume.

Results and Discussion

Voltammetry. The transport of $Fe(CN)_6^{3-}$ across the clay film was measured by its electrochemical reduction at the underlying platinum electrode when the potential is linearly swept over time between two potential limits +0.6 V and −0.2 V (SCE) in cyclic voltammetry, (Figure 1). It was shown that two types of diffusion,[9,10] linear and nonlinear, contribute to the voltammetric responses of $Fe(CN)_6^{3-}$ at the CME surface while a voltammetric response based on linear diffusion is usually observed with a rather large bare Pt electrode surface. To compare the solution diffusion (D_s) and the effective or apparent diffusion in clay film (D_c), experimental conditions were thus chosen where voltammetric responses are limited (1) by a linear diffusion process and (2) by a diffusion layer inside the clay film. This can be verified by varying the measurement sampling time (potential scan rate) and the deposited montmorillonite amount, i.e., the clay film thickness at the Pt electrode surface. The test is also performed in a 4 M NaCl bathing solution where the clay film thickness can be assumed to be thinnest i.e., under the lowest swelling conditions as discussed below. This allows the required experimental parameters used for the voltammetric investigations to be defined more precisely. The transition between nonlinear and linear diffusions[27] is characterized in cyclic voltammetry by the change from a plateau-shaped voltammogram of constant current intensity to a peak-shaped voltammogram whose current intensity (I_p) varies linearly with the square root of the potential scan rate, $v^{1/2}$. From the reported reduction current intensities plotted against $v^{1/2}$ in Figure 2, it can be shown that the transition occurs at lower potential scan rates or longer measurement time scales when the surface concentration of montmorillonite at the Pt surface increases. It must be noted that this peculiar voltammetric behavior of CME in the bathing electrolyte 4 M NaCl can be found with microchannel array electrodes.[28,29] A voltammetric response of CME based on a linear diffusion is thus found for potential scan rates, v, higher than 0.1, 0.05, and 0.02 V/s at respective coated montmorillonite concentrations of 0.28, 0.56, and 1.13 mg/cm^2. In the present work, a potential sweep rate of 0.05 V/s and surface concentration of 1.13 mg/cm^2 are the experimental parameters chosen to guarantee voltammetric detection based on a linear diffusion in the clay film.

Under these voltammetric detection conditions, I_p can thus be related to the concentration, c, of $Fe(CN)_6^{3-}$ in solution by the following general function

$$I_p = K\, c\, D^{1/2} v^{1/2} \tag{3}$$

where K is a characteristic voltammetric constant which includes the Pt electrode surface, the number of electrons involved in the redox mechanism, and D is the diffusion coefficient of $Fe(CN)_6^{3-}$ in the solution (D_s) or in the clay film (D_c).

The ratio, R, of current intensity obtained at CME ($I_{p_{CME}}$) and bare Pt electrode ($I_{p_{sol}}$) is used to measure the permeation properties of the clay films[9]

$$R = \frac{I_{p_{CME}}}{I_{p_{sol}}} \tag{4}$$

(27) Amatore, C.; Saveant, J.-M.; Tessier, D. *J. Electroanal. Chem.* **1983**, *147*, 39.

(28) Tokuda, K.; Morita, K.; Shimizu, Y. *Anal. Chem.* **1989**, *61*, 1763.

(29) Brumlik, C. J.; Martin, C. R.; Tokuda, K. *Anal. Chem.* **1992**, *64*, 1201

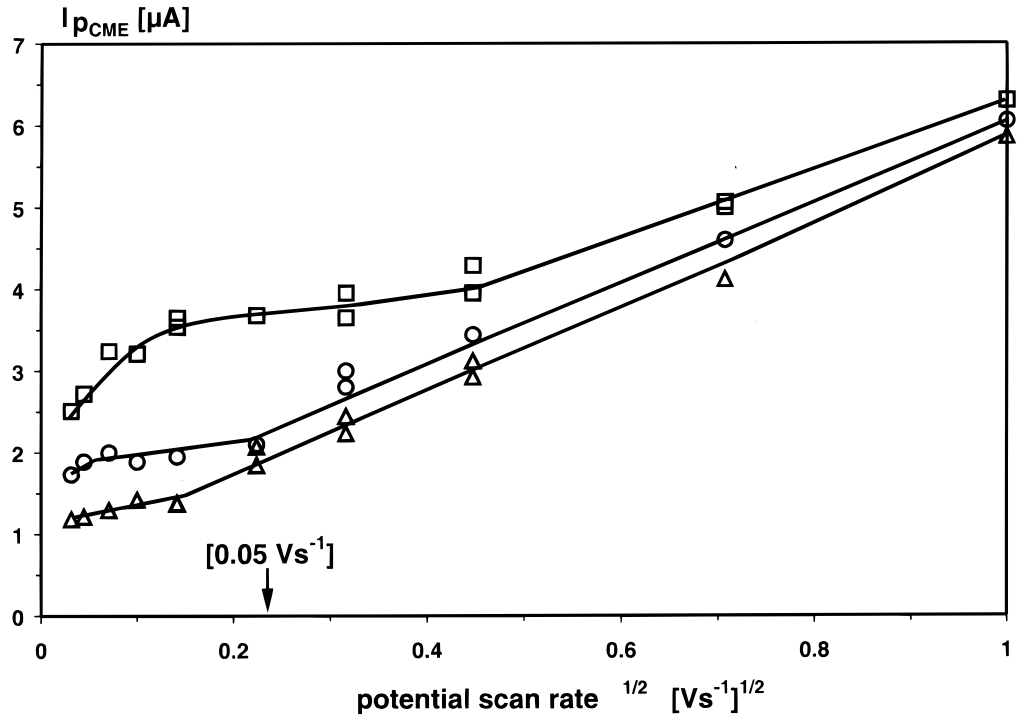

Figure 2. Effect of the potential scan rate on the reduction current intensity of $Fe(CN)_6^{3-}$ for various CME coatings in 4 M NaCl solution. □, CME coating 0.28 mg/cm²; ○, CME coating 0.56 mg/cm²; △, CME coating 1.13 mg/cm²; $K_3Fe(CN)_6$, 4 mM; Na-montmorillonite I.

In the case of of $Fe(CN)_6^{3-}$, an unretained electroactive molecule in the clay film, it can be assumed that the solution concentration c inside and outside the clay film does not vary.

According to eqs 3 and 4, the ratio of D_c to D_s, which expresses the relative variation of D in the clay film, is thus given by

$$R^2 = \frac{D_c}{D_s} \tag{5}$$

Salt Concentration Effect on the $Fe(CN)_6^{3-}$ Diffusion in CME. In most soils, anions which are not specifically adsorbed are in solution and are therefore mobile.[30] Their diffusion through the pore solution is thus characterized by a diffusion coefficient close to those measured in the free solution, D_s. However, in a porous medium with decreasing moisture, an apparent variation of D_s expressed in D_c is measured which depends on the cross-sectional area available for diffusion. Thus, the decrease of the porosity, Φ, and the increase of the diffusion path tortuosity are important retarding factors which limit the diffusion.

Clay Film Swelling. In the case of Na-montmorillonite, a dependence between the deposited film swelling and the water activity was established. It was shown that in the presence of water dry montmorillonite swells in a stepwise fashion with the introduction of water layers between plates,[22−24] also termed *intracrystalline swelling.* At a low water activity, a maximum stable plate separation of 1.9−2 nm is reached for the Na-montmorillonite crystal, which is caused by the hydration of the exchangeable cations in the interlayer. By increasing the water activity in the suspension, a sudden opening of the crystals occurs termed *osmotic swelling* where the basal spacing varies continuously. It results from the large concentration difference between ions located at the clay mineral surfaces and in the water solution. Thus, in a NaCl concentration range from 0.01 to 0.3 M, low-angle X-ray diffraction studies have shown that the average basal spacing d_{001} linearly increases with $c_s^{0.5}$, where c_s is the NaCl concentration in solution.[22]

It follows that changing the water activity either by drying or by changing the salt concentration would monitor the basal spacing of Na-montmorillonite. In Figure 3, the d_{001} basal spacings and the voltammetric results (R (4) and R^2 (5)) are compared in a NaCl solution concentration range from 0.02 to 4 M. The measured (crystalline swelling) d_{001} basal spacings between 0.5 and 4 M NaCl are reported. The average d_{001} basal spacing results (osmotic swelling) from Norrish et al.[22] in a NaCl solution concentration range from 0.02 to 0.2 M are also included for comparison. A decrease of these parameters is observed as the salt concentration increases, which is related to a higher compactness of montmorillonite plates in the clay films by decreasing the water activity. Thus, a shrinking of the clay film decreases $Fe(CN)_6^{3-}$ transport to the electrode surface. It must be remarked that similar R value variations have been obtained under experimental conditions where a preswelling step in the bathing electrolyte solution is performed.[9,12]

It has been considered that the long-range basal spacing of equilibrium between parallel-oriented single montmorillonite platelets or face−face interactions can determine the structural aspect of a Na-montmorillonite homogeneous film.[9] The void solution space between platelets corresponds to the film porosity which would control an intraparticle diffusion of the electrochemical marker. However, in the case of a trivalent anion such as $Fe(CN)_6^{3-}$, the electrostatic exclusion volume at the negatively charged surfaces of montmorillonite platelets, measured by twice the Debye length ($2/\kappa$),[31] as well as polarized

(30) Nye, P. H. *Adv. Agronomy* **1979**, *31*, 225.

(31) Pashley, R. M.; Quirk, J. P. *Soil Sci. Soc. Am. J.* **1997**, *61*, 58.

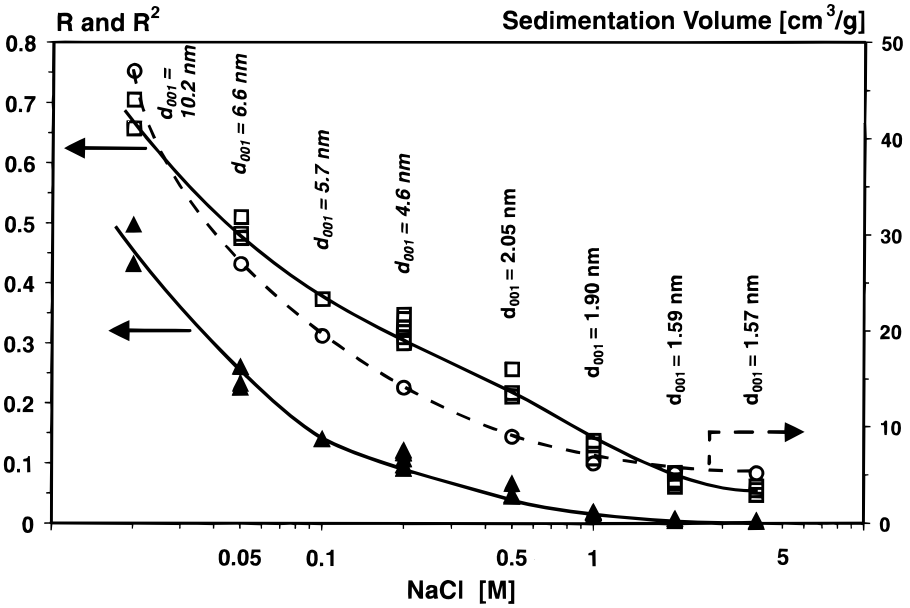

Figure 3. Effect of NaCl concentration on the montmorillonite clay sedimentation volume and cyclic voltammetric intensity current ratios $R = I_{pCME}/I_{psol}$ and R^2 (see Figure 1). d_{001} basal spacing values of Na-montmorillonite are also reported (see Methods section and text). □, R; ▲, R^2; ○, sedimentation volume; Na-montmorillonite I.

immobilized water layers of high viscosity (vicinal or surficial water), extending up to five monolayer thicknesses of water,[32] would occlude this pathway through the clay film.[30,33] An ideal Na-montmorillonite homogeneous film should thus be quasi-impermeable to the transport of $Fe(CN)_6^{3-}$ according to these electrostatic and hydration properties of the montmorillonite surface.

However, microscopic, spectroscopic, and sorption studies[34−38] give a more heterogeneous picture of the clay gel with an array of particles resulting from the heterogeneity of the surface density and the various bending potential of montmorillonite particles. Such arrangements could result in a discontinuous swelling of the CME film, in which interparticle pathways would control the permeability as discussed elsewhere.

Effective Porosity. To approach this CME film structure in contact with electrolyte solutions, the sedimentation volumes (V_{sed}) of concentrated montmorillonite solutions (10, 20, and 40 g/l Na-montmorillonite) were measured. In Figure 3, the average sedimentation volumes expressed in cm^3 of water per g clay are reported against the NaCl solution concentration and compared to the voltammetric results (R, R^2).

In the same way as for the d_{001} basal spacings, a decrease of V_{sed} is observed as the salt concentration in the solution increases, i.e., as the water activity decreases. In particular, it can be shown, in Figure 4, that a linear relationship exists ($r = 0.99$) between the sedimentation volumes and R^2 i.e., D_c/D_s which allows the following proposal to be made for approaching the clay film swelling effect on the $Fe(CN)_6^{3-}$ diffusion control.

By analogy to the dipping of the air-dried CME surface in the electrolyte solution, the solid clay has been directly mixed with the electrolyte solution for the measurement of sedimentation volumes. The relative variation of the long-time stabilized (six months) Na-montmorillonite sedimentation volumes is used to calculate an effective solution-filled porosity, Φ_e, of the clay film for $Fe(CN)_6^{3-}$. In this calculation, the extrapolated sedimentation volume $V_{sed}^{R^2=0}$ at $R^2 = 0$ would characterize an occluded compactness structure of the clay film which was taken as a reference state in the following relation

$$\Phi_e = \frac{V_{sed} - V_{sed}^{R^2=0}}{V_{sed}} \qquad (6)$$

It must be noted that V_{sed} given by the linear regression analysis when $R^2 \rightarrow 0$ matches the V_{sed} results obtained at salt concentrations higher than 1 M NaCl. Thus, the V_{sed} result obtained in 4 M NaCl was used for the calculation of Φ_e with eq 6.

In the following discussion, the D_c/D_s and Φ_e results obtained at $c_s \leq 1$M NaCl are thus considered. In Figure 5, the variation of the relative diffusion coefficient of $Fe(CN)_6^{3-}$ is reported against the so-derived efficient porosity Φ_e. As expected, a large decrease of D_c/D_s is observed as the calculated efficient porosity, Φ_e, nears zero, which has been further modeled.

Modeling. In the case of the conductance measurements of electrolyte solution-filled porous montmorillonite gels, a general way to understand the tortuosity effects on the ion diffusion is to consider the formation factor,[30] F. This measures the extent to which the solid particles reduce the specific conductance of the montmorillonite gels (k_{gel}) in relation to the solution (k_s), $F = k_s/k_{gel}$.

Empirical relations between porosity (Φ) and formation factor (F) including a tortuosity effect (τ) are generally established[11,30]

$$F \text{ function } (\Phi, \tau) \qquad (7)$$

In the case of montmorillonite gels, it was found that

(32) McBride, M. B.; Baveye, P. *Soil Sci. Soc. Am. J.* **1995**, *59*, 388.
(33) Olsen, S. R.; Kemper, W. D.; Van Schalk, J. C. *Soil Sci. Soc. Am. Proc.* **1965**, *29*, 154.
(34) Fripiat, J.; Cases, J.; François, M.; Lettelier, M. *J. Colloid Interface Sci.* **1982**, *89*, 378.
(35) Van Damme, H.; Levitz, P.; Fripiat, J. J.; Alcover, J. F.; Gatineau, L.; Bergaya, F. In *Physics of Finely Divided Matter*; Boccara, N., Daoud, D., Eds.; Springer-Verlag: Berlin, 1985; p 24.
(36) Cases, J. M.; Bérend, I.; Besson, G.; François, M.; Uriot, J. P.; Thomas, F.; Poirier, J. E. *Langmuir* **1992**, *8*, 2730.
(37) Morvan, M; Espinat, D.; Lambard, J.; Zemb, T. *Colloids Surf. A* **1994**, *82*, 193.
(38) Murray, R. S.; Quirk, J. P. *Soil Sci. Soc. Am. J.* **1990**, *54*, 1179.

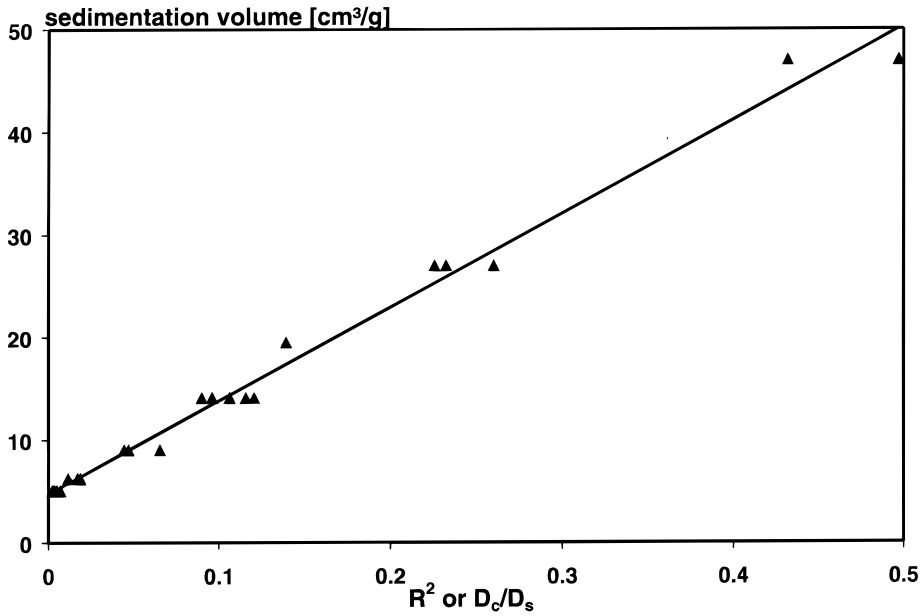

Figure 4. Relationship between the sedimentation volumes and the relative variation of the $Fe(CN)_6^{3-}$ diffusion coefficient at CME expressed in $R^2 = D_c/D_s$, (see also Figure 3).

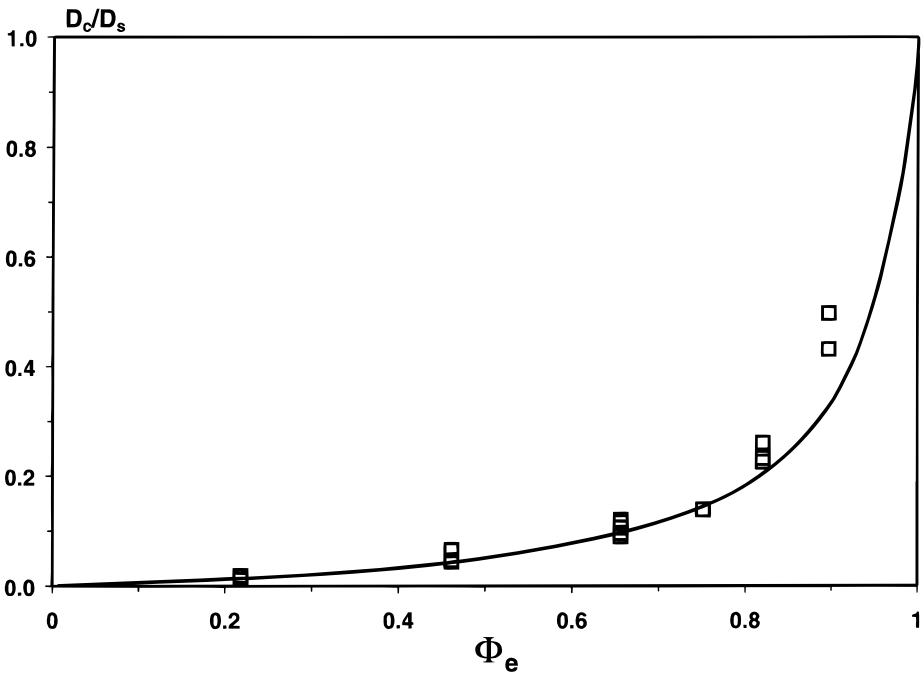

Figure 5. Dependence of the relative variation of $Fe(CN)_6^{3-}$ diffusion coefficient at CME, $R^2 = D_c/D_s$ on the effective porosity Φ_e (calculated with eq 6). The curve is calculated with eq 7 where the shape factor $\alpha = 17.8$ (see also text).

F is well described by a theoretical equation after Fricke[39] for the electric conductivity of solutions containing homogeneous spheroids

$$F = 1 + \alpha\frac{(1 - \Phi)}{\Phi} \qquad (8)$$

where α, the shape factor, depends on particles geometrical factors that account for the tortuosity effects. By assimiling montmorillonite particles to oblate spheroids (ellipsoid of revolution about minor axis B), satisfactory results have been obtained in establishing a relationship between the clay gel porosity, particle axial ratio, and the formation factor.[40−42]

In this work, a diffusion model based on the same theoretical approach was considered where F is set equal to D_s/D_c according to the Nernst−Einstein relation connecting the diffusion transport process and conductance.[43]

Knowing D_c/D_s from voltammetric measurements (eq 5), it follows that

(39) Fricke, H. *Phys. Rev*. **1924**, *24*, 575.

(40) Cremers, A.; Laudelout, H. *J. Chim. Phys.* **1965**, *62*, 1155.

(41) Dufey, J. E.; Laudelout, H. G. *J. Colloid Interface Sci.* **1975**, *51*, 278.

(42) Dufey, J. E.; Banin, A.; Laudelout, H. G.; Chen, Y. *Soil Sci. Soc. Am. J.* **1976**, *40*, 310.

(43) Kariuki, S.; Dewald, H. D. *Electroanalysis* **1996**, *8*, 307.

$$F = \frac{1}{R^2} = \frac{D_s}{D_c} = 1 + \alpha \frac{(1 - \Phi_e)}{\Phi_e} \quad (9)$$

where α only depends on the shape and orientation of the particles.

In the case of a random orientation of the oblate spheroids,[39] the shape factor α can be related to the axial ratio *A*/*B* of the particle with

$$\alpha = \frac{1}{3}\left(\frac{2}{1 - \frac{1}{2}M} + \frac{1}{M}\right) \quad (10)$$

where

$$M = \frac{\left(\rho - \frac{1}{2}\sin 2\rho\right)}{\sin^3\rho}\cos\rho \quad (11)$$

and

$$\cos\rho = \frac{B}{A} \quad (12)$$

with A = diameter of the particle and B = thickness of the particle.

For *A*/*B* values >5 in eqs 10, 11, and 12, a linear relationship exists between α and *A*/*B*.

$$\alpha = 0.982 + 0.212\,\frac{A}{B} \qquad (r^2 = 1) \quad (13)$$

It must be remarked that eq 10 obtained for oblate spheroids is a special case of a more general expression for an ellipsoid geometry which is defined along three axes *a*, *b*, and *c*. For the more simple geometry of oblate spheroid where $a = b = nc$ (n or $A/B > 1$); eq 10 giving the shape factor α can be discriminated into the following relations along the particle axis *a* and *b* (major axis *A*) and *c* (minor axis *B*).

For the case where the *A* axis is parallel to the $Fe(CN)_6^{3-}$ anion concentration gradient or perpendicular to the electrode surface, the shape factor α can be thus defined

$$\alpha = \frac{1}{1 - \frac{1}{2}M} \quad (14)$$

For *A*/*B* values > 1, it can be shown with eqs 11 and 12 that

$$\alpha \rightarrow 1 \text{ for } A/B > 1 \quad (15)$$

For the case where the *B* axis is parallel to the $Fe(CN)_6^{3-}$ anion concentration gradient or perpendicular to the electrode surface, it can be found that

$$\alpha = \frac{1}{M} \quad (16)$$

For *A*/*B* values >1, it can be calculated with eqs 11, 12, and 16 that

$$\alpha = 0.806 + 0.637\frac{A}{B} \qquad (r^2 = 1) \quad (17)$$

Equations 13, 15, and 17 between the shape factor α and the axial ratio *A*/*B* are reported in Figure 6.

In Figure 7, $F - 1$ results, as defined in eq 9, are plotted against $(1 - \Phi_e)/\Phi_e$. From the slope of the linear relationship, an average value $\alpha = 17.8 \pm 1$ ($r^2 = 0.95$) is calculated. In Figure 5, it can be shown that a constant shape factor describes the reported experimental results fairly well in the range of the calculated clay film effective porosities Φ_e from 0.2 to 0.8, i.e., under conditions of bathing electrolyte concentrations higher than 0.05 M NaCl.

According to eqs 13 and 17, the calculated shape factor $\alpha \gg 1$ also supposes that a large fraction of the particles are oriented to the electrode surface with the major axis *A* or the particle diameter lying parallel to the electrode surface (horizontal deposition). An estimation of the particles' *A*/*B* axial ratios in the clay film give values of 79 ± 5 and 27 ± 2, respectively for random and horizontal depositions. For comparison, the *A*/*B* axial ratio of highly dispersed Na-montmorillonite particles in water has been calculated from specific viscosities (η_{sp}) measurement. η_{sp} values of 0.019, 0.026, and 0.038 have been measured with 0.50, 0.67, and 1 g/l Na-montmorillonite solutions, respectively. An *A*/*B* axial ratio of 130 can be thus obtained with $[\eta] = 110$ and $\theta = 0$ in eqs 1 and 2.

It is obvious from the modeling in Figure 6 that a horizontal deposition (III) at the electrode surface of montmorillonite particles with a low axial ratio also hinders $Fe(CN)_6^{3-}$ transport, as in the case of randomly deposited particles (I) with a higher axial ratio.

In the case of spin-coating onto a small platinum electrode, a well-ordered clay film or gel can be formed where a horizontal deposition of montmorillonite particles prevails.[5,9] The rather constant α value found at bathing electrolyte concentrations higher than 0.05 M NaCl ($\Phi_e < 0.8$) supposes the presence of montmorillonite particles with a constant shape and orientation which will be discussed.

Thus, spectroscopic investigations of swelling smectite gels have established the existence of stable face-to-face aggregates (tactoids)[34−37] with a fairly constant size. They sustain the gel network which delimits swelling lenticular pores.[45] In solution, at electrolyte concentrations higher than 0.05 M NaCl, this close stacking of montmorillonite plates along the *B* axis (thickness) is also favored. A maximal stable basal spacing of about 2 nm characterizes the quasicrystalline nature of the tactoidal intraparticle structure (see crystalline swelling of Na-montmorillonite in Figure 3 and text). At low electrolyte concentrations, the osmotic swelling ensures a maximum plate separation giving rise to high basal spacing. However, the presence of stable tactoids is also widely documented[26,44] where the number of clay plates in the tactoids generally increases with the atomic weight and the charge of the exchangeable cation.

The formation of nonpermeable montmorillonite particles with a low axial ratio *A*/*B* can be also envisaged in the dense clay film structure of CME. The permeability of the clay film would thus depend on interparticle nonoccluded swelling pathways limited by domains with close-packed montmorillonite platelets, where an intraparticle or interlayer diffusive transport of $Fe(CN)_6^{3-}$ is excluded.[12] The fact that $Fe(CN)_6^{3-}$ diffuses through the clay film also indicates that the swelling volume is larger than the anion-exclusion and hydratation volumes extending at the montmorillonite surface. This can be related to the stiffness of the tactoidal structure which restricts a proper parallel alignment of the particles as would be

(44) Schramm, L. L.; Kwak, J. C. T. *Clays Clay Miner.* **1982**, *30*, 40.
(45) Keren, R.; Shainberg, I.; Klein, E. *Soil Sci. Soc. Am. J.* **1988**, *52*, 76.

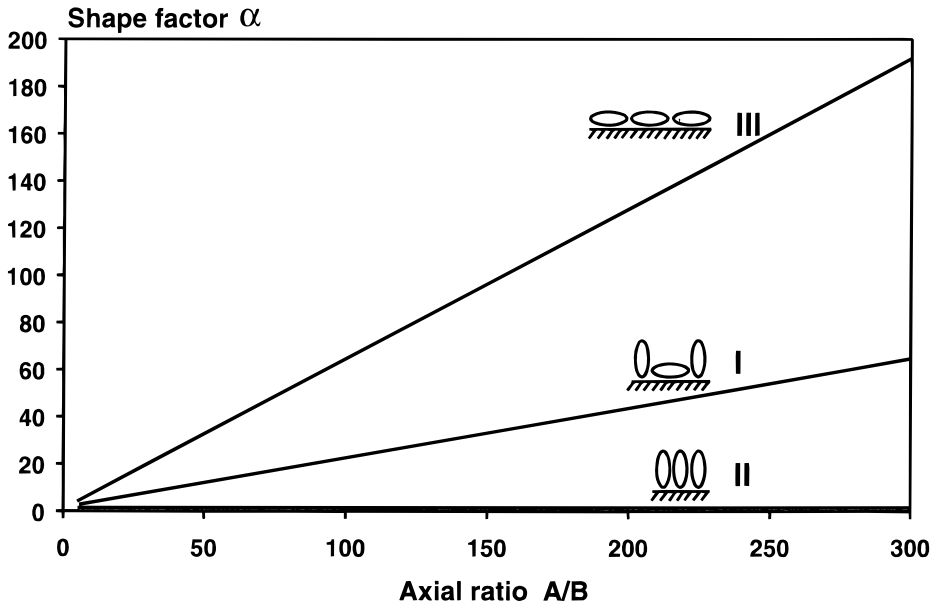

Figure 6. Effect of the particle orientation in a deposited film on the theoretical dependence between the shape factor α and the particle axial ratio *A*/*B* of the oblate spheroid (*A* ≫ *B*). I: random orientation, eq 13; II: perpendicular orientation of *A* axis, eq 15; III: parallel orientation of *A* axis, eq 17.

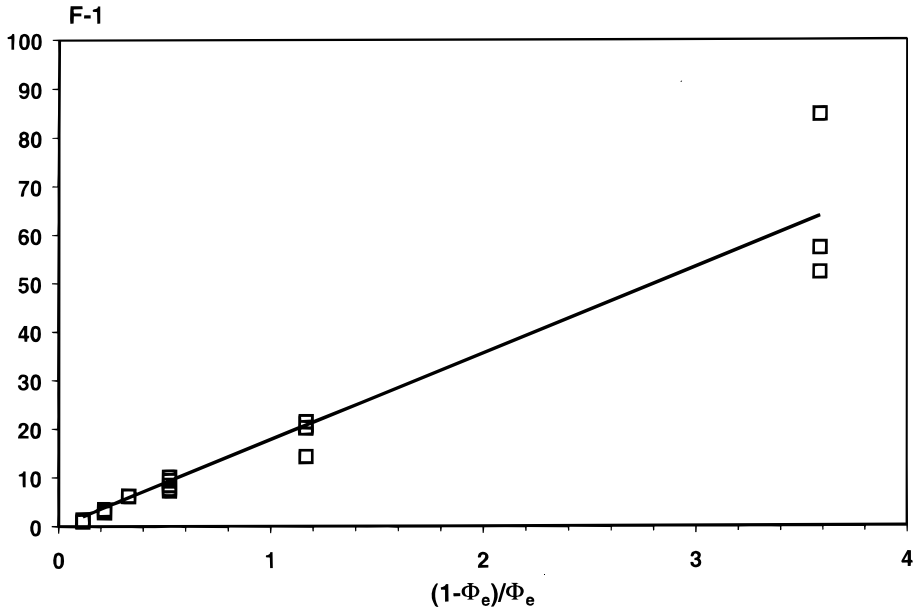

Figure 7. Linear regression analysis of the relation between the formation factor *F* and the effective porosity Φ_e according to eq 7.

found with highly flexible single montmorillonite platelets.[46] It results in a larger porosity.

At an effective porosity $\Phi_e > 0.8$, in Figure 5, higher D_c/D_s values than the simulated results are observed. Low α values can be calculated which indicate a more random orientation of the montmorillonite particles (Figure 6) probably due to three-dimensional edge-to-face interactions which prevail at NaCl concentrations lower than 0.05 M NaCl.[45] The presence of a foreign exchangeable cation such as K^+ from the 4 mM $K_3Fe(CN)_6$ solution during the clay swelling process could also increase the diffusion[47] through additional dislocation of the film under the conditions of low NaCl bathing concentrations.

In the same way, the measured R^2 values much smaller than 1% at 4 M NaCl (Figure 3) can be due to tactoid rearrangement during the weting and drying cycle of CME preparation. It results in intrinsic failures[38] which are detected by typical cyclic voltammetric responses for a microchannel electrode (Figure 2).

Effects of Water-Soluble Polymers. The strong interactions of polymers with clay minerals are due to multisite adsorption through the monomer units at the surface. It results in various modifications of clay mineral surface properties which mainly depend on the nature of the monomer functional groups and the polymer molecular weights. Polymers affect the aggregate stability of clay mineral and can thus modify the hydraulic conductivity of coating layered clay minerals structures. This has been investigated by measuring the $Fe(CN)_6^{3-}$ diffusion at CME previously modified by water-soluble synthetic polymers

(46) Van Damme, H.; Ben Ohoud, M. In *Disorder and Fracture*; Charmet, J. C., Roux, S., Eds.; Plenum Press: New York, 1990; p 105.
(47) Fitch, A.; Du, J.; Gan, H.; Stucki, J. W. *Clays Clay Miner.* **1995**, *43*, 607.

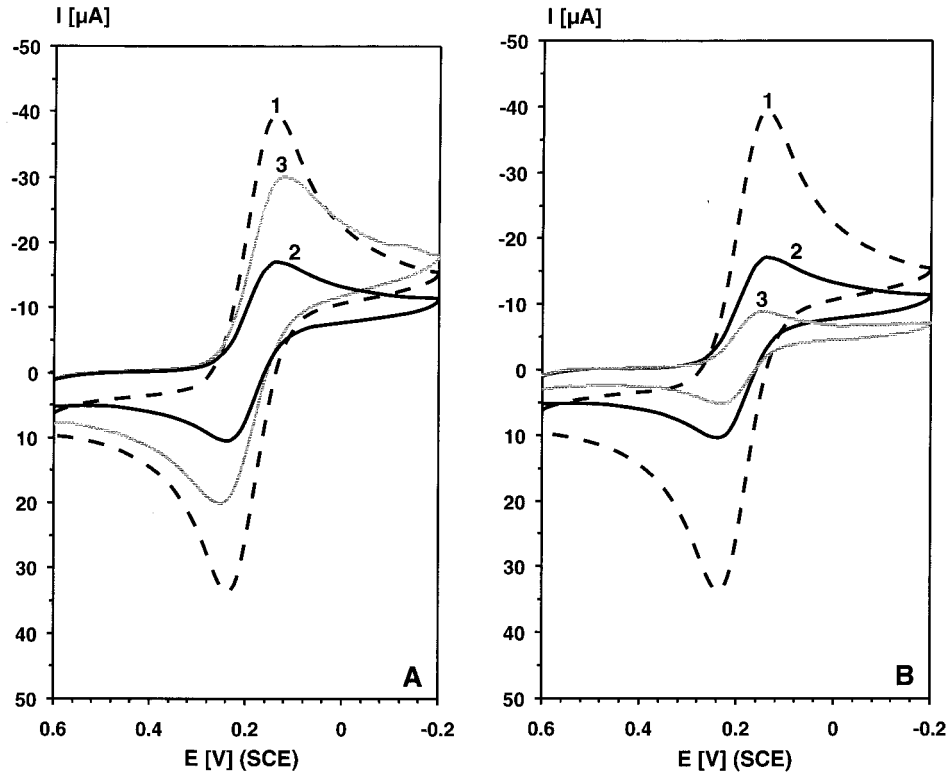

Figure 8. Cyclic voltammetric responses of $Fe(CN)_6^{3-}$ at polymer-modified CME (w/w: 5%) in 0.2 M NaCl solution. A: 1, bare-Pt electrode; 2, unmodified CME; 3, PAA (MW 2000 g/mol)-modified CME. B: 1, bare Pt electrode; 2, unmodified CME; 3, PVP (MW 44 000 g/mol)-modified CME. Potential scan rate 0.05 V/s; CME coating 1.13 mg/cm^2; $K_3Fe(CN)_6$, 4 mM; Na-montmorillonite II.

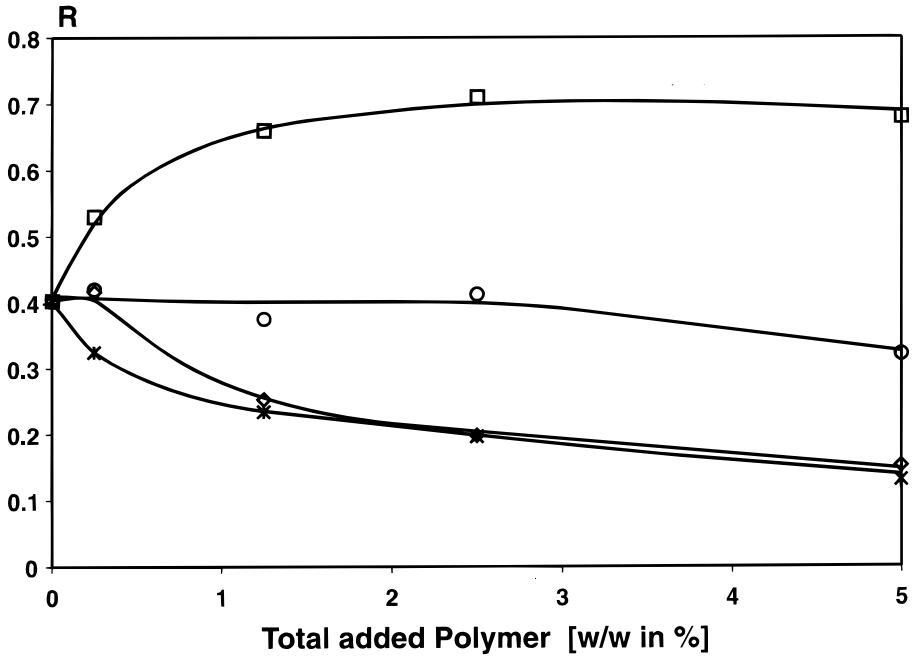

Figure 9. Effects of the water-soluble polymer content (w/w) of CME on the cyclic voltammetric intensity current ratios $R = I_{p_{CME}}/I_{p_{sol}}$ of $Fe(CN)_6^{3-}$ in 0.2 M NaCl solution. ○, PVP (MW 5000 g/mol); ∗, PVP (MW 44 000 g/mol); ◇, PVP (MW 400 000 g/mol); □, PAA (MW 2000 g/mol); Na-montmorillonite II.

of varying chemical compositions and molecular weights. In this study, polymers of a polyanionic character such as poly(acrylic acid) (PAA) as well as the nonionic polymer, poly(vinylpyrrolidone) (PVP), were considered.

Cyclic Voltammetric Results. Figure 8 shows typical cyclic voltammetric responses of $Fe(CN)_6^{3-}$ obtained with unmodified and polymer-modified CME in 0.2 M NaCl solution. It can be seen that a 5% (w/w) polymer modification of CME with PAA (MW 2000 g/mol) sensitively increases the intensity current (Figure 8, A) while the same percentage of modification with PVP (MW 44 000 g/mol) greatly decreases the cyclic voltammetric response (Figure 8B).

In Figure 9, the dependence of R (4) on the weight percentage of up to 5% (w/w) of added polymers in the Na-montmorillonite solution used for CME preparation is plotted. In a 0.2 M NaCl solution, the voltammetric results show an increase of R in the case of a CME

Table 1. Effects of Water-Soluble Polymers; Experimental Results and Modeling Parameters

water-soluble polymer (w/w: 5%)	sedimentation volume [cm^3/g]						$\bar{d}_z$ [μm](PCS)	
	0.2 M NaCl	4 M NaCl	Φ_e	R	$F = D_s/D_c$	α	water	0.2 M NaCl
without polymer	31	5.5	0.82	0.400	6.2	24	0.45	3
PAA (MW 2000 g/mol)	24	4	0.83	0.680	2.2	6	0.45	0.65
PVP (MW 5000 g/mol)	31.5	4.5	0.86	0.320	9.8	50	0.45	3
PVP (MW 44 000 g/mol)	18.8	4.5	0.76	0.135	55.5	173	0.75	4
PVP (MW 400 000 g/mol)	15	4	0.73	0.145	47.6	126	0.55	4

modification with a low-molecular-weight PAA (MW 2000 g/mol) polymer partially ionized at pH 5.6, while a decrease of R is observed for CME modification with different PVP molecular weights of 5000, 44 0000, and 400 000 g/mol. In the case of PVP, the voltammetric results also show a dependence of the polymer molecular weights used for CME modification. Thus, the presence of 1% PVP polymers of MW 44 000 g/mol or MW 400 000 g/mol in the CME more effectively decreases the relative current intensity R than a 5% addition of the PVP polymer with the lowest MW 5000 g/mol.

It must be noted that peak-shaped cyclic voltammetric responses of $Fe(CN)_6^{3-}$, in Figure 8, are always obtained with unmodified and polymer-modified CME in 0.2 M NaCl solution. They are proportional to the square root of the potential scan rate and are typical of a linear diffusion inside the clay film. The application of eq 3 for measuring a relative diffusion of $Fe(CN)_6^{3-}$, D_c/D_s, is thus applied and the variations of the formation factor F were used to characterize the polymer impact on the clay film structure.

Polymer Adsorption Behavior. Before discussing possible arrangements of the clay domains in the coated montmorillonite layer, some information about the adsorption characteristics of the polymers must be briefly reviewed. Under the solution concentration conditions used for CME preparation, it can be considered that the polymer adsorption at the montmorillonite surface is quasi-total.[48−50,52] In the case of PAA, it has been shown that the adsorption of negatively ionized polycarboxylic polymer is electrostatically hindered at the permanent negatively charged siloxane plate surface. However specific binding of polycarboxylate at aluminol sites of the edge surface can take place through a ligand exchange mechanism.

In the case of the nonionic PVP polymer, an overall adsorption at montmorillonite surfaces occurs. The building of the flocculated polymer/montmorillonite structure is possible where PVP polymers are layered between the siloxane plates.[51]

Modeling Parameters. Taking into account these polymer adsorption characteristics, the modifications of the clay film permeability are now discussed with the help of the modeling results.

Voltammetric and sedimentation volumes results were moreover considered for the case of a 5% addition of polymers (PAA and PVP) in the deposited clay film at the platinum electrode. The sedimentation volumes obtained under 4 M NaCl salt solution conditions were also taken as a reference state for the calculation of an effective porosity Φ_e with eq 6.

In Table 1, sedimentation volumes, Φ_e, R, F or D_s/D_c, and α calculated with eq 9 are reported for comparison. A rapid overview shows that no correlation can be found between the shape factor α and the effective porosity Φ_e after the different polymer modifications of the CME. Thus, in a small range of effective porosities, $\Phi_e = 0.80 \pm 0.06$, calculated α values vary from 6 to 173. According to the results expressed in eqs 13 and 17 in Figure 6, such a dispersion of the shape factor values can be modeled by various orientations and axial ratios of montmorillonite particles in the clay film.

In the case of the PAA modification, for a constant A/B axial ratio value, the decrease of α would indicate a more vertical deposition of the CME film. On the other hand, in the case of a fixed particle orientation in the clay film, the reduction of α could be related to a decrease of the axial ratio A/B values.

A contrasting behavior for the arrangement of the clay particles in the CME film can be now assumed after PVP modification. The increase of α would indicate either a more horizontal deposition of the clay film if the axial ratio remains constant or an increase of the axial ratio A/B in the case of an unmodified orientation of particles.

These interpretations are restricted to a single parameter variation. It is clear that simultaneous variations of the two α-determining parameters, particle orientation and axial ratio, can also be considered. Therefore, an attempt was made to specify some major parameter variations from other experimental results.

Sedimentation Volume and Photon Correlation Spectroscopic Results. In the presence of polymers, the decrease of the sedimentation volumes of montmorillonite particles supposes a collapse of the montmorillonite gel network. However, measurements (Table 1) with photon correlation spectroscopy (PCS) of the polymer-modified montmorillonite particles in 0.2 M NaCl show marked differences in their hydrodynamic behaviors. Thus, an average hydrodynamic diameter value, $\bar{d}_z$, of about 3 μm can be calculated for unmodified montmorillonite particles under salt-induced aggregation conditions. In the presence (w/w, 5%) of the low-molecular-weight PAA (MW 2000 g/mol), a decrease of $\bar{d}_z$ value down to 0.65 μm is now observed for montmorillonite aggregates. On the other hand, the aggregate size of PVP-modified montmorillonite samples remains high. A $\bar{d}_z$ value of 4 μm can be calculated for PVP (MW 44 000 g/mol)-modified montmorillonite (w/w, 5%) sample. For comparison, in a salt-free water solution, $\bar{d}_z$ values of 0.45 μm are calculated for unmodified and PAA-modified montmorillonite particles. In the case of PVP (MW 44 000 g/mol)-modified montmorillonite particles, a $\bar{d}_z$ value of 0.75 μm is also calculated.

Modeling Results. The permeability properties of the polymer-modified clay films can be thus modeled according to these salt and polymer effects on particle size.

In the case of PVP modification, the variation of the average hydrodynamic particle diameter can be related to the flocculating effect of PVP. At low PVP adsorbed amounts, a partial overlapping of the platelets along the major axis A can be observed. A horizontal deposition and a concomitant increase of the A/B axial ratio are therefore parameter variations which lengthen the interparticle diffusing path for $Fe(CN)_6^{3-}$ ions. The molecular weight dependence of the shape factor α also shows that this

(48) Blockhaus, F.; Séquaris, J.-M.; Narres, H. D.; Schwuger, M. J. *J. Colloid* Interface Sci. **1997**, *186*, 234.
(49) Hild, A.; Séquaris, J.-M.; Narres, H. D.; Schwuger, M. J. *Colloids Surf. A* **1997**, *123−124*, 515.
(50) Bassmann, F.; Séquaris, J.-M.; Narres, H. D.; Schwuger, M. J. *J. Dispersion Technol.* **1999**, *20(1&2)*, 607.
(51) Francis, C. W. *Soil Sci.* **1973**, *115*, 40.
(52) Séquaris, J.-M.; Bassmann, F.; Hild, A.; Narres, H. D.; Schwuger, M. J. *Colloids Surf. A* **1999**, *159* (2&3), 503−512.

band-type network of particles is favored by PVP of high molecular weights which flocculate montmorillonite particles more easily by a bridging mechanism than a PVP of low molecular weight.

In the presence of a low-molecular-weight PAA (MW 2000 g/mol), a decrease of the sedimentation volume also supposes a better packing of the montmorillonite particles. However, as shown by the PCS results, the aggregate size of the particle in 0.2 M NaCl is limited after interaction with the low molecular weight PAA. This probably results from an electrostatic stabilization due to the screening of the positively charged montmorillonite edge surface which otherwise favors aggregations through edge interactions. A slight increase of the negative electrophoretic mobility also confirms the overall negativate trend of the montmorillonite particles in the presence of PAA.[50] This surface charge homogeneity would favor a more parallel alignment of the individual montmorillonite platelets in a condensed film phase. Indeed, X-ray diffraction results[22,53] have shown that a highly ordered parallel alignment for clay platelets can be observed in the presence of other oxyanions such as phosphate compounds which interact in a similar way through specific bindings at the edge of clay minerals.[48] A stacking of clays platelets in straight columns rather than in a random or zigzag columns, Figure 10, has been proposed from the XRD results. In the case of the CME modified by PAA MW 2000 g/mol, the diminution of the shape factor α in Table 1 can also be associated with the formation of close-packing domain structures with a lower *A*/*B* axial ratio. Thus, the negatively repelling charged surfaces of the particle quasicrystalline structure would delimit shorter interparticle diffusing paths to the electrode surface for $Fe(CN)_6^{3-}$.

Conclusions

This voltammetric study of the montmorillonite clay film permeability not only shows the importance of a salt-dependent film porosity but also supports the presence of occluded clay domains. The modeling of the diffusion-controlled transport of $Fe(CN)_6^{3-}$ is based on macroscopic sedimentation data which allow an effective porosity of the clay film to be approached. Transport through a montmorillonite layer is also limited by the heterogeneity of the clay film due to particles formed from stacking platelets which exclude permeant anions. During the swelling process, the arrangement of these less flexible particles than single montmorillonite platelets creates larger pores. The presence of adsorbed organic polymers can affect the orientations and axial ratios of these particles in different ways depending on their nature, concentrations and molecular weights. This may already result in the establishment of preferential pathways[54] via interparticles governing anion transport. Thus, voltammetric results can give some insights into the behavior of swelling clay in soils where interactions with electrolytes and organic matter as well as drying−weting cycles are known to affect the soil permeability through the development of preferential pathways.

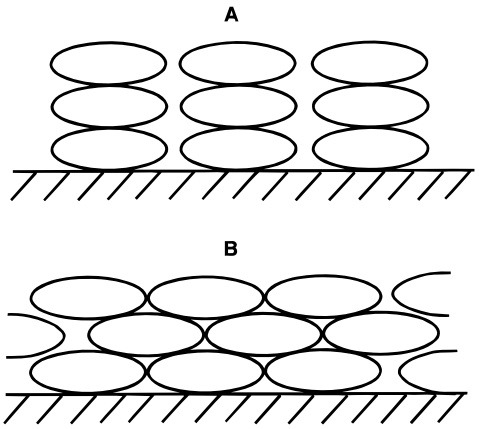

Figure 10. Models for stacking oblate spheroids in straight column (A) or in zigzag column (B).

Acknowledgment. Thanks are due to C. Walraf for technical assistance.

LA990550E

(53) Tateyama, H.; Scales, P. J.; Ooi, M.; Nishimura, S.; Rees, K.; Healy, W. T. *Langmuir* **1997**, *13*, 2440.

(54) Yaron, B.; Calvet, R.; Prost, R. *Soil Pollution*; Springer: Berlin, 1996; Chapter 8.